A standardized catalog of 225 MgII absorption-selected galaxies: correlations, covering fractions, and cantankerous outliers

Nikole M. Nielsen[1], C.W. Churchill[1], G.G. Kacprzak[2]

[1]New Mexico State University, [2]Swinburne University of Technology

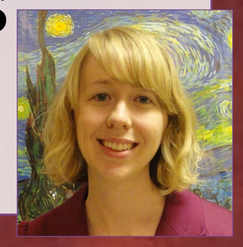

Introduction & Motivation

Inflowing and outflowing gas in galaxy halos is important in star formation. Such gas is diffuse and extended, and, therefore, difficult to observe directly. Background quasars (QSOs) are excellent probes of these halos, which can be studied via their associated absorption profiles in QSO spectra. The MgII λλ2796, 2803 doublet can be observed at optical wavelengths over the redshift range $0.3 \le z \le 2.5$ and is commonly used to determine gaseous halo properties. Many previous surveys have been published with samples no larger than ~80 galaxies. In many cases, galaxy magnitudes, colors, and QSO-galaxy projected separations are not directly comparable between surveys due to differing cosmologies and magnitude systems. It is desirable to standardize previous surveys to form a large uniform sample of MgII absorption-selected galaxies.

Data Collection & Method

We conducted an extensive literature search for MgII absorption-selected galaxies and built a catalog of 225. For each galaxy we have the measured apparent magnitudes, color, projected separation from the QSO beam (impact parameter, D), and the MgII equivalent width, $W_r(2796)$.

We have standardized all galaxy properties to the current ΛCDM cosmology and all B-band and K-band absolute magnitudes to the AB system using uniform *k*-corrections (see Kim 1996) and the SEDs of Mannucci et al. (2001). B-K colors were calculated from absolute magnitudes or converted from a B-R color using a linear relation: (B-R)=0.49(B-K)+0.12.

We identified group and isolated galaxies where a group galaxy is defined as having a nearest neighbor within 100 kpc (projected on the sky) and having a velocity separation no greater than 500 km s^{-1}. All other galaxies are considered isolated. Of 225 galaxies, 193 are isolated. For 80 we have high resolution spectra from HIRES/Keck or UVES/VLT in order to study kinematics at ~6km s^{-1}. We also have 32 group galaxies of which 12 have HIRES/UVES spectra.

Sample

We present our standardized galaxy sample in Figures 1 and 2. In Figure 1, impact parameter (D) is plotted against galaxy redshift (z_{gal}). Point colors represent different $W_r(2796)$ bins (see legend). Figure 2 presents three dimensional distributions of QSO-galaxy D, galaxy B-band luminosity (L_B), and absolute K magnitude (M_K). Galaxy types were assigned based on the following color cuts:

Early	(B-K) ≥ 1.76
Late	1.16 < (B-K) < 1.76
Irregular	(B-K) ≤ 1.16

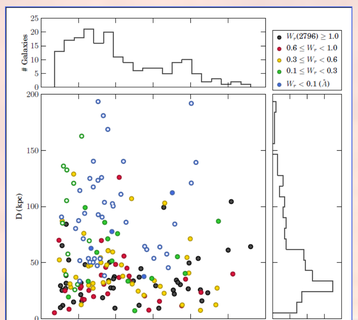

Figure 1 Redshift and Impact Parameter
Colored points indicate different $W_r(2796)$ bins (see legend). Open points represent galaxies which have limits for $W_r(2796)$.

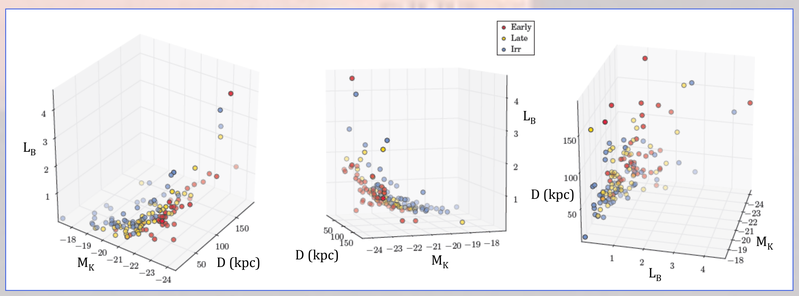

Figure 2 Distribution of the Sample
The sample is shown in three different orientations for L_B vs M_K vs D. Data points are color coded by galaxy type (see legend). Only galaxies with measured colors are plotted.

Galaxy Colors

We examined whether the rest-frame galaxy color B-K evolves over redshift. Figure 3 plots B-K and B-R colors against galaxy redshift for different $W_r(2796)$ bins as indicated in the legend. We ran a Kendall-tau rank correlation test on B-K vs z_{gal}.

With a significance less than 2σ, **no color evolution was found**.

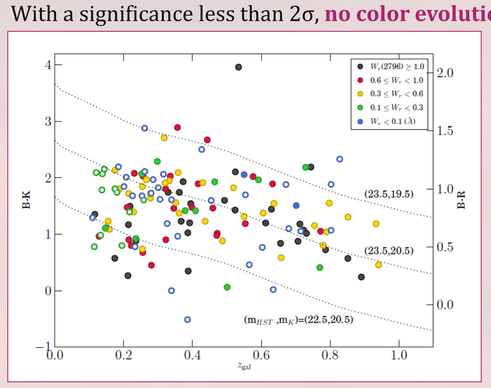

B-K vs z_{gal} rank correlation test
τ = -0.11
P(τ) = 0.0427
CL = 95.473%
N(σ) = 2.0

Figure 3 Color Evolution
Galaxy rest-frame B-K and B-R colors versus redshift for various $W_r(2796)$ bins. Open points represent galaxies which have limits for $W_r(2796)$. Dotted lines provide contours of constant apparent magnitudes.

$W_r(2796)$ & Impact Parameter

In Figure 4a, we plot $W_r(2796)$ against D for isolated galaxies. ***$W_r(2796)$ for isolated galaxies is anti-correlated with D at the 7.8σ level*** (accounting for limits). This indicates that the quantity of halo gas diminishes with projected distance. We found that a log-linear fit was the best parameterization for this anti-correlation (see fit parameters in figure). The standard deviation of the data around the fit is σ = 0.72. Visually, it appears that each galaxy type may follow a different log-linear fit; further analysis to come.

Figure 4b shows **for a given $W_r(2796)$, group galaxies tend to be located at all D**, indicating that the quantity of gas in groups is more extended than around isolated galaxies.

A 2D Kolmogorov-Smirnov test between $W_r(2796)$ and D for isolated and group galaxies indicates that **isolated and group galaxies are not drawn from the same population** (KS=0.41, P(KS)=10^{-3}, CL = 99.889%) .

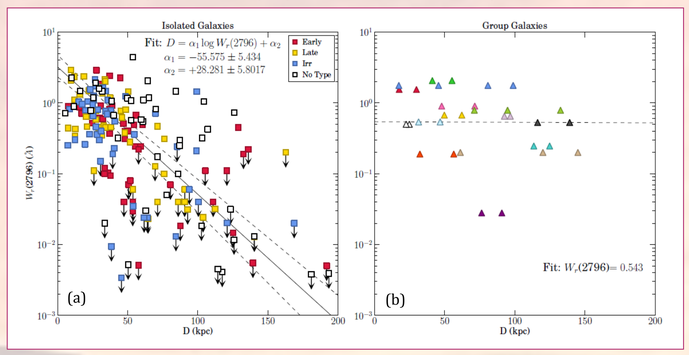

Figure 4 Absorption Line Strength vs Impact Parameter
(a) Isolated galaxies. Galaxy types are represented by colors (see legend). The solid line is a log-linear maximum likelihood fit to the data and the dashed curves provide 1σ uncertainties. (b) Group galaxies. Different point colors represent different groups. The dashed line is a linear fit consistent with a null slope, showing no anti-correlation with D.

Absorption Gas Kinematics

Figure 5 presents the $W_r(2796)$ absorption profiles as a function of D for 50 galaxies in which $W_r(2796)$ was detected in HIRES/UVES spectra. We modeled the gas kinematics using Voigt profile fits. The models are presented as red profiles. Galaxies with a limit in $W_r(2796)$ are not shown, but these additional 30 galaxies can provide further insights to the patchiness (covering fraction) of halos when included. Further detailed analysis to come.

Luminosity Scaling & Covering Fractions

The extent of absorbing gas is commonly assumed to follow a Holmberg-like relation, $R(L) = R_*(L/L_B^*)^\beta$. We examined whether the halo gas radius also depends on absorption strength, $W_r(2796)$. We adopted four $W_r(2796)$ cuts and obtained R_* and β by maximizing the number of galaxies with $W_r(2796) \ge W_{cut}$ below the fitted line and maximizing the number of galaxies with $W_r(2796) < W_{cut}$ above the fitted line. Results are presented in Figure 6. **The luminosity scaling steepens from β ~ 0.3 to β ~ 0.4 at W_{cut} = 0.6 Å. R_* is on the order of 70 kpc, possibly decreasing for W_{cut}= 1 Å. The covering fraction decreases with W_{cut}.**

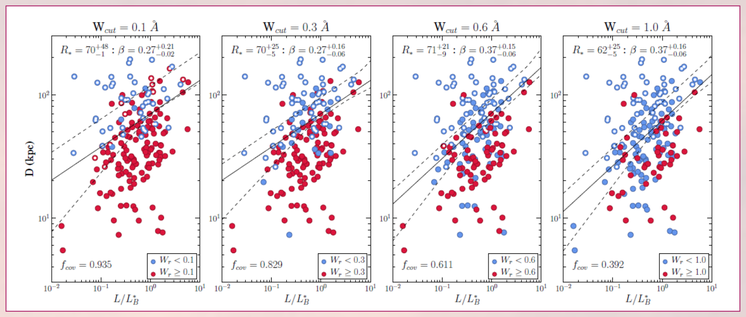

Figure 6 Impact Parameter vs Luminosity for Different $W_r(2796)$ Bifurcations
In each panel, blue points are galaxies that have a measured $W_r(2796) < W_{cut}$ and red points are galaxies with $W_r(2796) \ge W_{cut}$. Open points represent galaxies which have limits for $W_r(2796)$. R_* and β give the fit parameters and f_{cov} gives the covering fraction for each bifurcation. Dashed lines provide the 1σ uncertainties in the fit.

We compared the luminosity scaling between early and late type galaxies for W_{cut}=0.3 Å, which we illustrate in Figure 7.

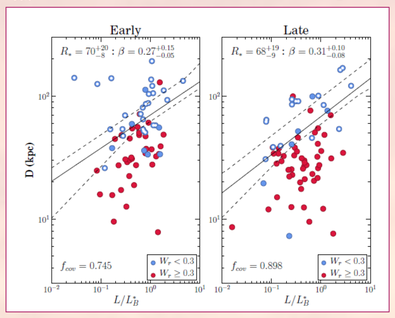

The luminosity dependence of the halo gas radius is identical regardless of galaxy type (based on color), though late types may have a slightly large covering fraction.

Figure 7 Impact Parameter vs Luminosity for Early and Late Type Galaxies
Open points represent galaxies which have limits for $W_r(2796)$.

Conclusions & Future Work

- No color evolution was found.
- Gas in isolated galaxy halos diminishes with distance while gas in group galaxy halos does not.
- Luminosity scaling steepens and covering fraction decreases for increasing W_{cut} but neither have dependence on galaxy type.

We will continue our study of absorption gas kinematics for isolated and group galaxies. This involves including galaxies with limits for $W_r(2796)$ and determining if the kinematics depend on D, galaxy luminosity and/or galaxy color. We will also compare the distribution functions of cloud column densities, thermal widths, and the two-point velocity function between isolated and group galaxies.

References

Kim, S., Goobar, A., & Perlmutter, S. 1996, PASP, 108, 190

Mannucci, F., Basile, F. Poggianti, B. M., Cimatti, A., Daddi, E., Pozzetti, L., & Vanzi, L. 2001, MNRAS, 326, 745

The following papers were included in our literature search:

Chen, H.-W., Helsby, J. E., Gauthier, J.-R., Shectman, S. A., Thompson, I. B., & Tinker, J. L. 2010, ApJ, 714, 1521

Chen, H.-W., & Tinker, J. L. 2008, ApJ, 687, 745

Churchill, C. W., Kacprzak, G. G., Nielsen, N. M., Steidel, C. C., & Murphy, M. T. 2011, ApJ, submitted

Guillemin, P., & Bergeron, J. 1997, A&A, 328, 499

Kacprzak, G. G., Churchill, C. W., Barton, E. J., & Cooke, J. 2011, ApJ, 733, 105

Kacprzak, G. G., Churchill, C. W., Evans, J. L., Murphy, M. T., & Steidel, C. C. 2011, MNRAS, 416, 3118

Kacprzak, G. G., Murphy, M. T., Churchill, C. W. 2010, MNRAS, 406, 445

Steidel, C. C., Dickinson, M., Meyer, D. M., Adelberger, K. L., & Sembach, K. R. 1997, ApJ, 480, 568

Steidel, C. C., Dickinson, M., & Persson, S. E. 1994, ApJ, 437, L75

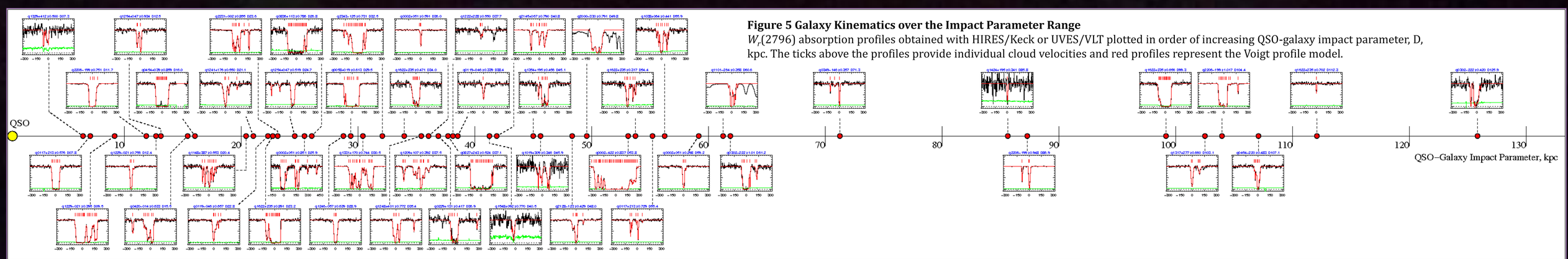

Figure 5 Galaxy Kinematics over the Impact Parameter Range
$W_r(2796)$ absorption profiles obtained with HIRES/Keck or UVES/VLT plotted in order of increasing QSO-galaxy impact parameter, D, kpc. The ticks above the profiles provide individual cloud velocities and red profiles represent the Voigt profile model.